BEST AVAILABLE IMAGES

Defective images within this document are accurate representations of the original documents submitted by the applicant.

Defects in the images may include (but are not limited to):

- BLACK BORDERS
- TEXT CUT OFF AT TOP, BOTTOM OR SIDES
- FADED TEXT
- ILLEGIBLE TEXT
- SKEWED/SLANTED IMAGES
- COLORED PHOTOS
- BLACK OR VERY BLACK AND WHITE DARK PHOTOS
- GRAY SCALE DOCUMENTS

IMAGES ARE BEST AVAILABLE COPY.

As rescanning documents *will not* correct images, please do not report the images to the Image Problem Mailbox.

Journal of Neurochemistry
Raven Press, Ltd., New York

Overexpressed Monomeric Human Acetylcholinesterase Induces Subtle Ultrastructural Modifications in Developing Neuromuscular Junctions of *Xenopus laevis* Embryos

Shlomo Seidman, Revital Ben Aziz-Aloya, Rina Timberg, Yael Loewenstein, *Baruch Velan, *Avigdor Shafferman, †Jian Liao, ‡Bent Norgaard-Pedersen, †Urs Brodbeck, and Hermona Soreq

*Department of Biological Chemistry, Hebrew University of Jerusalem, Jerusalem; *Department of Biochemistry, Israel Institute for Biological Research, Ness-Ziona, Israel; †Institute of Biochemistry and Molecular Biology, University of Bern, Bern, Switzerland; and ‡Statens Seruminstitut, Copenhagen, Denmark*

Abstract: Formation of a functional neuromuscular junction (NMJ) involves the biosynthesis and transport of numerous muscle-specific proteins, among them the acetylcholine-hydrolyzing enzyme acetylcholinesterase (AChE). To study the mechanisms underlying this process, we have expressed DNA encoding human AChE downstream of the cytomegalovirus promoter in oocytes and developing embryos of *Xenopus laevis*. Recombinant human AChE (rHAChE) produced in *Xenopus* was biochemically and immunochemically indistinguishable from native human AChE but clearly distinguished from the endogenous frog enzyme. In microinjected embryos, high levels of catalytically active rHAChE induced a transient state of overexpression that persisted for at least 4 days postfertilization. rHAChE appeared exclusively as nonassembled monomers in embryos at times when endogenous *Xenopus* AChE displayed complex oligomeric assembly. Nonetheless, cell-associated rHAChE accumulated in myotomes of 2- and 3-day-old embryos within the same subcellular compartments as native *Xenopus* AChE. NMJs from 3-day-old DNA-injected embryos displayed fourfold or greater overexpression of AChE, a 30% increase in postsynaptic membrane length, and increased folding of the postsynaptic membrane. These findings indicate that an evolutionarily conserved property directs the intracellular trafficking and synaptic targeting of AChE in muscle and support a role for AChE in vertebrate synaptogenesis.
Key Words: Neuromuscular junction—*Xenopus laevis* embryos—Human acetylcholinesterase—Muscle.
J. Neurochem. **62**, 1670–1681 (1994).

Formation of a functional neuromuscular junction (NMJ) requires the targeted deposition of synaptic proteins at the nerve–muscle interface (Flucher and Daniels, 1989; Froehner, 1991; Ohlendieck et al., 1991). Among these proteins is the acetylcholine-hydrolyzing enzyme acetylcholinesterase (AChE), responsible for terminating cholinergic neurotransmission across the NMJ (Hall, 1973). It is not yet clear how the selective accumulation of synapse-specific proteins at the NMJ is accomplished. One mechanism for achieving synaptic localization of AChE is probably the compartmentalized transcription and translation of AChE mRNA (Rotundo, 1990; Rossi and Rotundo, 1992). Aggregation and anchoring of AChE at the postsynaptic cell surface are mediated by evolutionarily conserved components of the synaptic basal lamina, such as heparan sulfate proteoglycans (Brandan et al., 1985) and agrin (McMahan, 1990). Similar mechanisms appear to be involved in the biosynthesis of the nicotinic acetylcholine receptor (AChR) (Changeux, 1991; Phillips et al., 1991; Wallace, 1991) and may represent a general solution to the problem of localizing junctional proteins in muscle cells (Pavlath et al., 1989; Ralston and Hall, 1989). However, the molecular determinants controlling the intracellular transport of AChE and the elements specifying its synaptic localization in muscle remain to be elucidated.

In the developing *Xenopus laevis* embryo, muscle differentiation, primitive neuromuscular contacts, and spontaneous synaptic activity are observed within 1 day postfertilization (PF) (Kullberg et al., 1977). During the ensuing 24 h, ultrastructural specializations characterizing synaptic differentiation are observed, followed by the acquisition of spontaneous

Received July 14, 1993; revised manuscript received September 16, 1993; accepted September 16, 1993.
Address correspondence and reprint requests to Dr. H. Soreq at Department of Biological Chemistry, Hebrew University of Jerusalem, Jerusalem, 91904, Israel.

Abbreviations used: AChE, acetylcholinesterase; ACHE, acetylcholinesterase gene; AChR, acetylcholine receptor; CMV, cytomegalovirus; CMVACHE, acetylcholinesterase cDNA downstream of the cytomegalovirus promoter–enhancer element; mAb, monoclonal antibody; NMJ, neuromuscular junction; PF, postfertilization; rHAChE, recombinant human acetylcholinesterase.

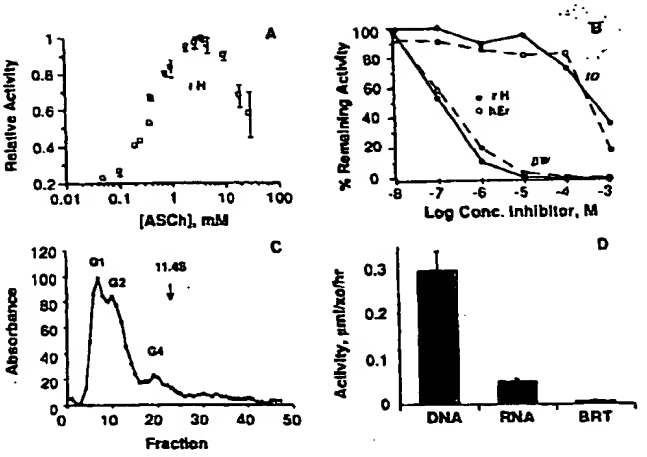

FIG. 1. *Xenopus* oocytes express catalytically active rHAChE. **A:** Inhibition by excess substrate. Mature *Xenopus* oocytes were injected with 5 ng of in vitro-transcribed AChE mRNA (Soreq et al., 1990) and incubated overnight at 17°C. Homogenates corresponding to one-third oocyte were assayed for AChE activity in the presence of various concentrations of acetylthiocholine (ASCh) substrate [average of three experiments ± SEM (bars)]. **B:** Sensitivity to selective inhibitors. Oocyte homogenates were preincubated for 30 min in assay buffer containing the AChE-specific, reversible inhibitor 1,5-bis(4-allyldimethylammoniumphenyl)-pentan-3-one dibromide [BW284C51 (BW)] or the butyrylcholinesterase-specific inhibitor tetraisopropylpyrophosphoramide (IO) at the indicated concentrations and assayed for remaining activity following addition of 2 mM ASCh. Data are averages of duplicate assays from two independent microinjection experiments. AChE extracted from human erythrocytes (hEr) served as control. rH, rHAChE. **C:** Oligomeric assembly. Homogenates from ACHE mRNA-injected oocytes were subjected to sucrose density centrifugation as described in Materials and Methods. Data are averages of thr e experiments. Note that in addition to the free monomer (3.2S; G1), the oocyte appears to generate dimers (5.6S; G2) and to a lesser extent tetramers (10.2S; G4) of human AChE. Endogenous oocyte AChE activity is undetectable under these conditions. The arrow marks the position of bovine liver catalase (11.4S). **D:** Expression of ACHE DNA in *Xenopus*. Oocytes were injected with 5 ng of synthetic ACHE mRNA or CMVACHE (Velan et al., 1991*a*) and incubated for 1 (RNA) to 3 (DNA) days. Oocytes injected with incubation medium (BRT) or uninjected oocytes serv d as control. Activity is expressed as micromoles of substrate hydrolyzed per hour per oocyte, in mean ± SEM (bars) values for three independent microinjection experiments.

motor activity and hatching (Cohen, 1980). Fervent embryonic development and ultrastructural maturation of the neuromuscular system continue, giving rise to a free swimming tadpole within 4–5 days. From day 2 PF, a steady increase in AChE activity is observed (Gindi and Knowland, 1979), concomitant with a developmentally regulated decrease in the time course of the synaptic potential in *Xenopus* myotomes (Kullberg et al., 1980). The rapid development of the neuromuscular system in *Xenopus* thus makes it an excellent in vivo model for the study of vertebrate myogenesis and synaptogenesis.

We have cloned a DNA sequence encoding human AChE and used it to express catalytically active AChE in microinjected *Xenopus* oocytes (Soreq et al., 1990) and cultured human cells (Velan et al., 1991*a*). Placed downstream f either the native human AChE gene (ACHE) promoter or the cytomegalovirus (CMV) enhancer–promoter and introduced into fertilized *Xenopus* eggs, this DNA led to overexpression of AChE in NMJs of 2-day-old embryos (Ben Aziz-Aloya et al., 1993). Here, we present a biochemical and histochemical characterization of this recombinant human AChE (rHAChE) as expressed in *Xenopus*. Moreover, we demonstrate the persistence of overexpressed enzyme in NMJs to at least day 3 of embryonic development and offer evidence indicating subtle alterations in the ultrastructure of NMJs from embryos overexpressing rHAChE. Our findings indicate the assignment of catalytically active monomeric rHAChE to subcellular compartments common to those occupied by native, multimeric *Xenopus* AChE in embryonic myotomes and suggest a morphogenetic role for AChE in vertebrate synaptogenesis.

MATERIALS AND METHODS

In vitro fertilization and microinjections

DNA microinjections into *X. laevis* oocytes and fertilized eggs were essentially as previously described (Ben Aziz-

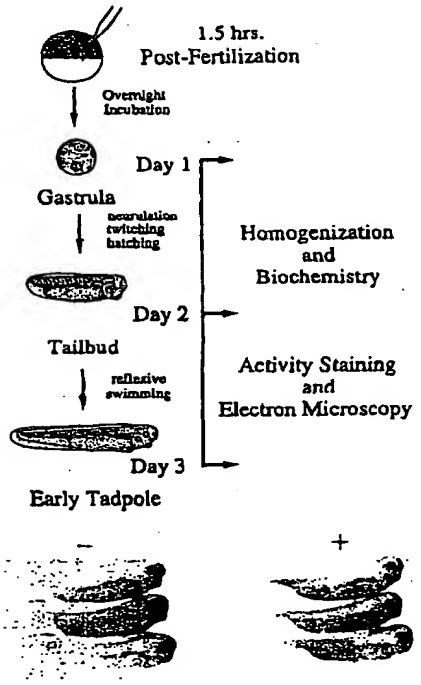

FIG. 2. Normal development of CMVACHE-injected embryos. A schematic representation of a microinjection experiment depicting the principal developmental stages and analytical approaches used in this work is shown together with photographs displaying the normal gross development of unstained microinjected embry s (+) compared with control uninjected embryos (–) 3 days PF. In vitr f rtilized eggs of *Xenopus laevis* were injected with 1 ng of CMVACHE and cultured for 1–4 days as described in Materials and Methods. Sketches are modeled after those of Deuchar (1966).

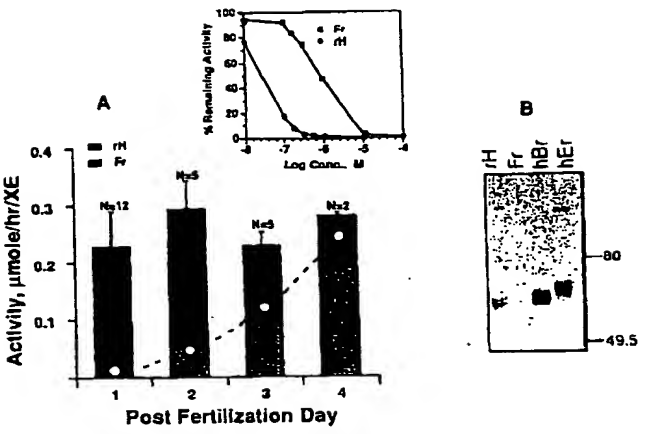

FIG. 3. CMVACHE-injected *Xenopus* embryos express and maintain biochemically distinct heterologous human AChE for at least 4 days. A: Overexpression of rHAChE in developing embryos. High-salt/detergent extracts of CMVACHE-injected and uninjected embryos were prepared and assayed for AChE activity in the presence and absence of the selective inhibitor echothiophate (3.3×10^{-7} *M*; inset). Endogenous AChE activity was calculated according to an algorithm assuming 90% inhibition of rHAChE and 20% inhibition of frog AChE at this concentration of inhibitor. The bar graph represents the total AChE activity measured per microinjected embryo at various time points following microinjection and the calculated activities attributable to rHAChE (dark shading) and endogenous frog AChE (light shading). The total AChE activity measured in uninjected control embryos at the same time points is indicated by open circles. Data represent average ± SEM (bars) values from four to six embryos from the indicated number (N) of independent microinjection experiments. Inset: Selective inhibition of rHAChE by echothiophate. Homogenates representing endogenous frog (Fr) or recombinant human (rH) AChE were assayed for activity following a 40-min preincubation with the indicated concentrations of echothiophate. Data are averages of three experiments. B: Immunochemical discrimination between rHAChE and embryonic *Xenopus* AChE. Affinity-purified AChE from CMVACHE-injected *Xenopus* embryos (rH), control uninjected embryos (Fr), human brain (hBr), and erythrocytes (hEr) was subjected to denaturing gel electrophoresis and protein blot analysis as described in Materials and Methods. Each lane represents ~20 ng of protein, except rH, which contained only 6 ng. Note the complete absence of immunoreactivity with embryonic *Xenopus* AChE, although silver staining of a parallel gel demonstrated detectable protein at the corresponding position (data not shown). The faint upper bands (140–160 kDa) in the lanes displaying native human AChEs represent dimeric forms resulting from incomplete reduction of the intersubunit disulfide bonds (see Liao et al., 1992). Prestained molecular weight markers indicated on the right were from Bio-Rad, U.S.A..

Aloya et al., 1993). Fertilized eggs were dejellied with 2% cysteine and injected within the first two cleavage cycles in medium containing 5% Ficoll in 0.3× Mark's modified Ringer (MMR). Several hours after microinjection, embryos were transferred into 0.3× MMR and cultured overnight at 17–19°C. One-day-old embryos were transferred to either 0.1× MMR or aged tap water and cultured for an additional 1–3 days.

Activity assays

Embryos were harvested in groups of three to five apparently normal individuals and stored frozen until used. Homogenates were prepared in a high-salt/detergent buffer [0.01 *M* Tris, 1.0 *M* NaCl, 1% Triton X-100, and 1 m*M* EGTA (pH 7.4); 150 μl per embryo] and assayed for enzymatic activity as detailed elsewhere (Neville et al., 1992). For subcellular fractionations, groups of three embryos were homogenized in low-salt buffer [0.02 *M* Tris-HCl (pH 7.5), 0.01 *M* $MgCl_2$, and 0.05 *M* NaCl; 100 μl per embryo] and centrifuged at 100,000 rpm for 10 min in a Beckman model TL100 tabletop ultracentrifuge. The supernatant was collected and considered the low-salt-soluble fraction. The pellet was resuspended in low-salt/detergent buffer [0.01 *M* phosphate buffer (pH 7.4) and 1% Triton X-100], incubated on ice for 1 h, and centrifuged as above for 5 min to generate the detergent-soluble fraction. The remaining pellet was resuspended in high-salt buffer [0.01 *M* phosphate buffer (pH 7.4), 1.0 *M* NaCl, and 1 m*M* EGTA] to release the high-salt-soluble AChE fraction.

Protein blot analyses

rHAChE was purified by affinity chromatography from ~180 "day 1" embryos injected with plasmid DNA carrying AChE cDNA downstream of the CMV promoter–enhancer element (CMVACHE) using a modified procedure for the purification of native human AChE (Gennari and Brodbeck, 1985). In brief, AChE from embryos homogenized in low-salt/detergent buffer was bound to Sepharose beads carrying *N*-(1-amino-hexyl)-3-dimethylethylaminobenzoic amide by shaking overnight at room temperature. Elution was with 0.02 *M* edrophonium chloride (Tensilon; Hoffmann-La Roche, Basel, Switzerland). Embryonic *Xenopus* AChE was similarly purified from 1-week-old tadpoles but had to be eluted by boiling in 0.1% sodium dodecyl sulfate. Denaturing sodium dodecyl sulfate–polyacrylamide gel electrophoresis and blotting were essentially as described elsewhere (Liao et al., 1992) using a pool of monoclonal antibodies (mAbs; 132-1,2,3; 6 μg/ml each) raised against denatured human brain AChE (Brodbeck and Liao, 1992).

Sucrose gradient analysis of AChE subunit assembly

Freshly prepared, high-salt/detergent extracts from one or two embryos or five to 10 oocytes were applied to 12-ml 5–20% linear sucrose density gradients and centrifuged overnight at 4°C. Fractions were collected into 96-well mi-

TABLE 1. *Subcellular fractionation of rHAChE in CMVACHE-injected* Xenopus *embryos*

	rH			
Fraction	Day 1	Day 2	Day 3	Fr (day 3)
LSS	57 ± 2	60 ± 4	53 ± 3	36 ± 5
DS	37 ± 2	34 ± 4	36 ± 3	31 ± 4
HSS	6 ± 2	5 ± 1	10 ± 1	33 ± 7

Fertilized *Xenopus* eggs were microinjected with 1 ng of CMVACHE DNA, cultured for 1–3 days, and subjected to homogenization and subcellular fractionation as described in Materials and Methods. rHAChE in each fraction (rH) was detected by enzyme–antigen immunoassay (Liao et al., 1992) using a specific mAb (101-1) raised against bovine brain AChE. Endogenous AChE activity in uninjected tadpoles (Fr) was determined by the standard colorimetric assay described in Materials and Methods. Percent enzyme activity in each fraction (average ± SEM) is shown for three to five groups of three embryos from a single microinjection experiment. LS, low-salt soluble; DS, detergent soluble; HSS, high-salt soluble.

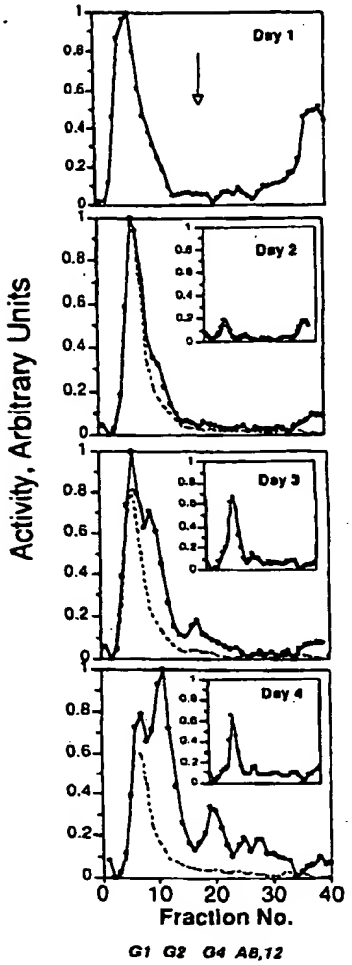

FIG. 4. rHAChE in microinjected *Xenopus* embryos remains monomeric. High-salt/detergent extracts representing two embryos were subjected to sucrose density centrifugation as described in Materials and Methods. Shown are total AChE (solid line) and immunoreactive rHAChE (dotted line) from CMVACHE-injected embryos 1–4 days PF. rHAChE appeared exclusively as a peak representing monomeric AChE (~3.2S) at all time points. The arrow marks the position of bovine liver catalase (11.4S). Insets: AChE molecular forms in control uninjected embryos scaled to the total activity levels observed in DNA-injected embryos (see Fig. 2). Peak analysis demonstrated that the distribution of oligomeric forms was identical to that observed in CMVACHE-injected embryos. Note that monomeric AChE is essentially undetectable in control embryos. G1, G2, and G4 indicate the expected positions of the globular monomer, dimer, and tetramer in the gradient; A8 and 12 indicate the positions of "tailed" asymmetric forms. Fraction 0 represents the top of the gradient.

crotiter plates and assayed for total AChE activity as previously described (Soreq et al., 1989). To distinguish between rHAChE and endogenous *Xenopus* AChE in gradient fractions, 100-μl aliquots were transferred to a Maxisorp immunoplate (Nunc, Copenhagen, Denmark) coated with an mAb (mAb 101-1) recognizing human but not frog AChE and diluted 1:1 with double distilled water. Following overnight incubation, the plates were washed three times with phosphate-buffered saline containing 0.05% Tween 20, and each well was assayed for catalytically active AChE.

Cytochemical AChE staining and electron microscopy

Embryos were fixed, cytochemically stained for AChE, and prepared for electron microscopy as previously described (Ben Aziz-Aloya et al., 1993). Cytochemical staining (Karnovsky, 1964) was carried out in acetate buffer (pH 6.1) for 15–20 min at 4°C within 3 days of fixation.

RESULTS

Xenopus-expressed AChE is biochemically indistinguishable from native human AChE

Microinjected into mature *X. laevis* oocytes, 5 ng of in vitro-transcribed AChE mRNA directed the production of catalytically active AChE displaying substrate and inhibitor interactions characteristic of the native human enzyme (Fig. 1A and B). The apparent K_m calculated for rHAChE toward acetylthiocholine was 0.3 m*M*, essentially identical to that displayed by rHAChE expressed in cell lines (Velan et al., 1991*a*) and native human erythrocyte AChE (data not shown). In sucrose density centrifugation rHAChE sedimented primarily as monomers and dimers, although a discernible peak apparently representing globular tetrameric AChE was also observed (Fig. 1C). When CMVACHE (Velan et al., 1991*a*) was microinjected into oocytes, active AChE in yields 10–20-fold higher than that observed following RNA injections was obtained (Fig. 1D), demonstrating efficient transcription from this promoter in *Xenopus*.

Transient expression of CMVACHE in *Xenopus* embryos

Microinjected into cleaving *Xenopus* embryos, CMVACHE directed the biosynthesis of rHAChE at levels similar to those observed in DNA-injected oocytes. Yet, the gross morphology and development of CMVACHE-injected embryos appeared completely normal (Fig. 2). Moreover, gross motor function of microinjected embryos, as evaluated by twitching and hatching on day 2, reflexive swimming on day 3, and free swimming on later days, was unimpaired compared with normal, uninjected controls. Microinjected tadpoles survived up to 4 weeks, showing no overt developmental handicaps (data not shown). Following overnight incubation, at which time embryos had reached the late gastrula stage, endogenous AChE levels were negligible, and rHAChE activity represented a 50–100-fold excess over normal (Fig. 3A). From day 2 PF, detectable endogenous AChE activities increased steadily. Using the irreversible AChE inhibitor echothiophate (Neville et al., 1992) to distinguish between endogenous frog AChE and rHAChE (Fig. 3A, inset), we observed the persistence of receding levels of rHAChE for at least 4 days PF. For the first 3 days rHAChE accounted for >50% of the total measured AChE activity in microinjected embryos and resulted in a state of general overexpression com-

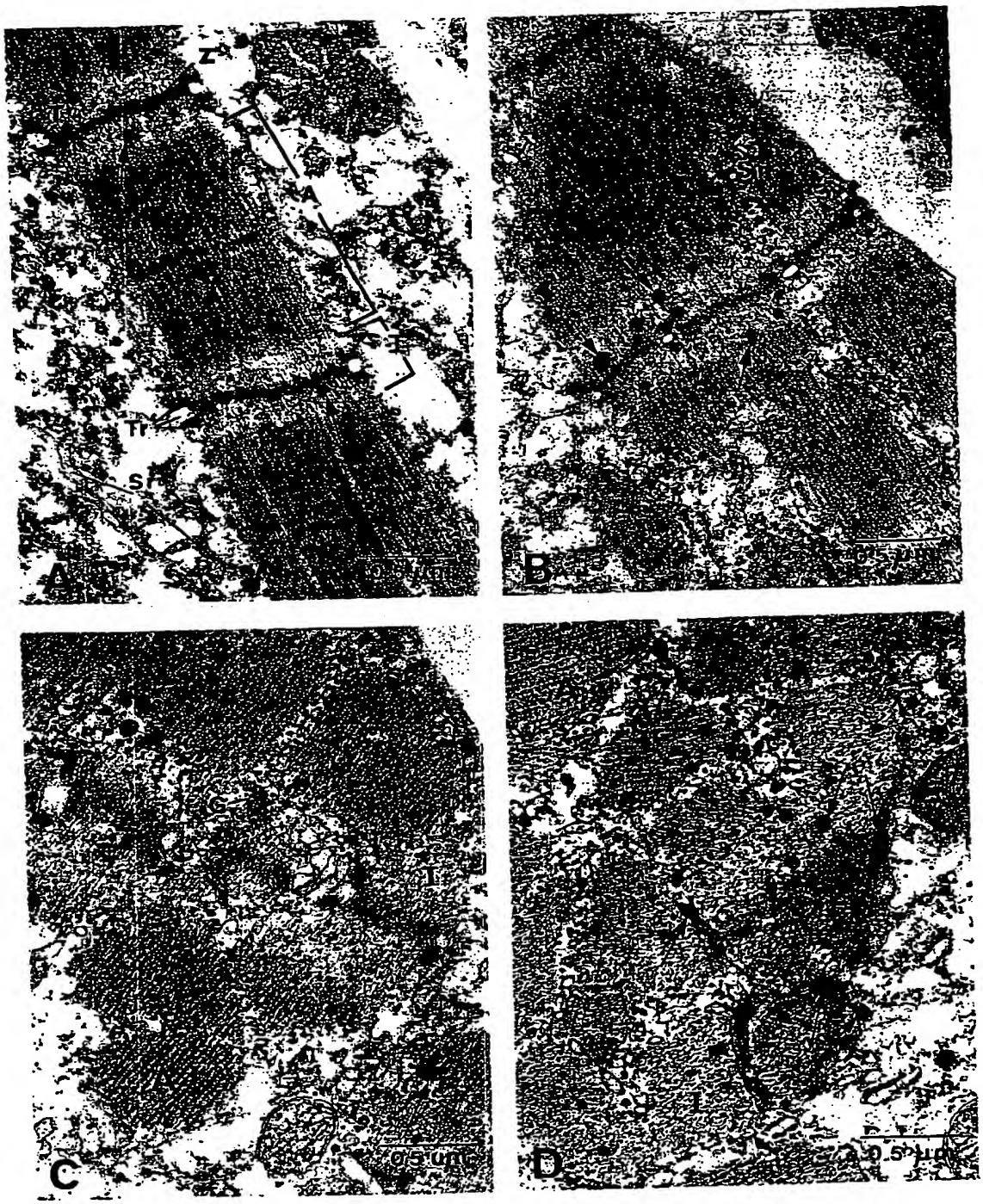

FIG. 5. Disposition of rHAChE in myotomes from 2-day-old microinjected *Xenopus* embryos. Fertilized *Xenopus* eggs were microinjected with 1 ng of CMVACHE, incubated for 2 days at 17°C, fixed, stained, and prepared for electron microscopy as described in Materials and Methods. Uninjected embryos from the same fertilization served as controls and were similarly treated. Arrows mark accumulations of reaction product indicating sites of catalytically active AChE. **A:** Uninjected control myotome in longitudinal section following activity staining for AChE. **B:** Myotome section from CMVACHE-injected embryo. **C:** Uninjected control myotome in transverse section. **D:** Transverse section from CMVACHE-injected embryo. Note the increased intensity of staining in sections from injected embryos versus uninjected controls within the same subcellular compartments, especially within the sarcoplasmic reticulum (Sr). A, A band; I, I band; Z, Z disc; Tr, triad; T, T tubules; G, glycogen particles. Bar = 0.5 μm.

pared with uninjected controls. By day 6 PF, no heterologous enzyme could be detected in homogenates (data not shown). At all time points examined, the level of frog AChE in CMVACHE-injected tadpoles appeared less than that observed in uninjected embryos.

In immunoblot analysis following denaturing gel electrophoresis, rHAChE was observed to comigrate with native human brain AChE, yielding a clearly visible doublet band at ~68 kDa (Fig. 3B). rHAChE was selectively recognized by a pool of mAbs raised against denatured human brain AChE, and no cross-immunoreactivity with embryonic *Xenopus* AChE was observed (Fig. 3B). The doublet band observed may reflect differences in glycosylation (Kronman et al., 1992). Sequential extractions with low-salt, detergent, and high-salt buffers revealed that ~35% of rHAChE synthesized in transiently transgenic embryos was associated with membranes, requiring detergent for solubilization (Table 1). Whereas up to 33% of the endogenous enzyme in day 3 uninjected tadpoles appeared in the high-salt-extractable fraction, salt-soluble rHAChE remained primarily in the low-salt fraction at all days examined (Table 1). Enzyme-antigen immunoassay with a species-specific mAb (mAb 101-1) was used to differentiate between human and frog enzyme in the fractions.

rHAChE remains monomeric in *Xenopus* embryos

To examine the possibility that heterologous human AChE could undergo homomeric oligomeric assembly or interact with either catalytic or noncatalytic subunits of *Xenopus* AChE to produce hybrid oligomers, sucrose density centrifugation and enzyme–antigen immunoassay were performed. At all time points examined, we observed rHAChE exclusively as nonassembled monomers sedimenting at ~3.2S, despite the concomitant accumulation of various multimeric forms of the endogenous frog enzyme (Fig. 4). When oligomeric AChE purified from CMVACHE-transfected cell cultures (Velan et al., 1991*b*) or from human brain (Liao et al., 1992) was preincubated with extracts of day 3 uninjected embryos and similarly analyzed, monomers, dimers, and tetramers were detected, and the distribution of oligomeric forms observed was identical to that in control samples (data not shown). Thus, mAb 101-1 detects all the globular configurations of rHAChE, and proteolytic activity does not appear to degrade stable oligomeric AChE in embryo extracts. Endogenous *Xenopus* AChE appeared primarily as a dimer on day 2 PF with globular tetrameric and asymmetric tailed forms appearing and increasing in content from day 3 onward (Fig. 4, insets). Superposition of the gradients from control and CMVACHE-injected embryos demonstrated that the normal developmental progression of *Xenopus* AChE oligomeric assembly was conserved in CMVACHE-injected embryos despite the high excess of rHAChE monomers (Fig. 4 and data not shown).

Subcellular dispositi n f rHAChE in myotomes f CMVACHE-injected embryos

Whole-mount cytochemical staining of CMVACHE-injected embryos indicated accumulation of AChE in myotomes 2 days PF (data not shown). We therefore undertook an ultrastructural analysis, at the electron microscope level, of myotomes from 2- and 3-day-old embryos microinjected with CMVACHE as compared with normal uninjected controls. Longitudinal and transverse sections from rostral trunk somites revealed clearly discernible myofibers 2 days PF in both injected and uninjected embryos (Fig. 5). By day 3 PF, both groups displayed significant increases in their numbers of myofibrillar elements and in maturation of the sarcoplasmic reticulum (Fig. 6). To examine the subcellular localization of nascent AChE in transgenic and control embryos, we used cytochemical activity staining (Karnovsky, 1964). In both the experimental and control groups, crystalline deposits of electron-dense reaction product were observed primarily in association with myofibrils, among the myofilaments, and within the sarcoplasmic reticulum (Figs. 5 and 6). Various organelles, including the nuclear membrane, free and bound polyribosomes, Golgi, and sometimes mitochondria, were also stained (Figs. 5 and 6 and data not shown).

At day 2 PF, staining in CMVACHE-injected embryos was conspicuously more pronounced than that observed in uninjected controls, in both the quantity and intensity of reaction product (Fig. 5). However, variability was observed between tissue blocks, probably reflecting mosaic expression of the injected DNA and/or variability in the efficiency of expression between embryos (S.S. and H.S., unpublished data). In longitudinal sections from CMVACHE-injected embryos, staining appeared to be concentrated at the I band of myofibers, particularly around the triad marking the intersection of the sarcoplasmic reticulum and T-tubule systems. In contrast, the sparse staining observed in control sections appeared randomly distributed. By day 3 PF, the general staining intensity in both groups had significantly increased, whereas observable differences between the groups were less dramatic. Cross sections revealed especially prominent staining within the sarcoplasmic reticulum (Fig. 6A and B). Strong staining was now observed at both the A and I bands and, for the first time, within the T-tubules (Fig. 6C and D). Overall, day 2 CMVACHE-injected myotomes resembled day 3 uninjected control myotomes in staining incidence and intensity (Figs. 5A and C and 6B and D).

Ultrastructural consequences of overexpressed AChE in *Xenopus* NMJs

We have previously demonstrated up to 10-fold overexpression of catalytically active AChE in NMJs of CMVACHE-injected embryos 2 days PF (Ben

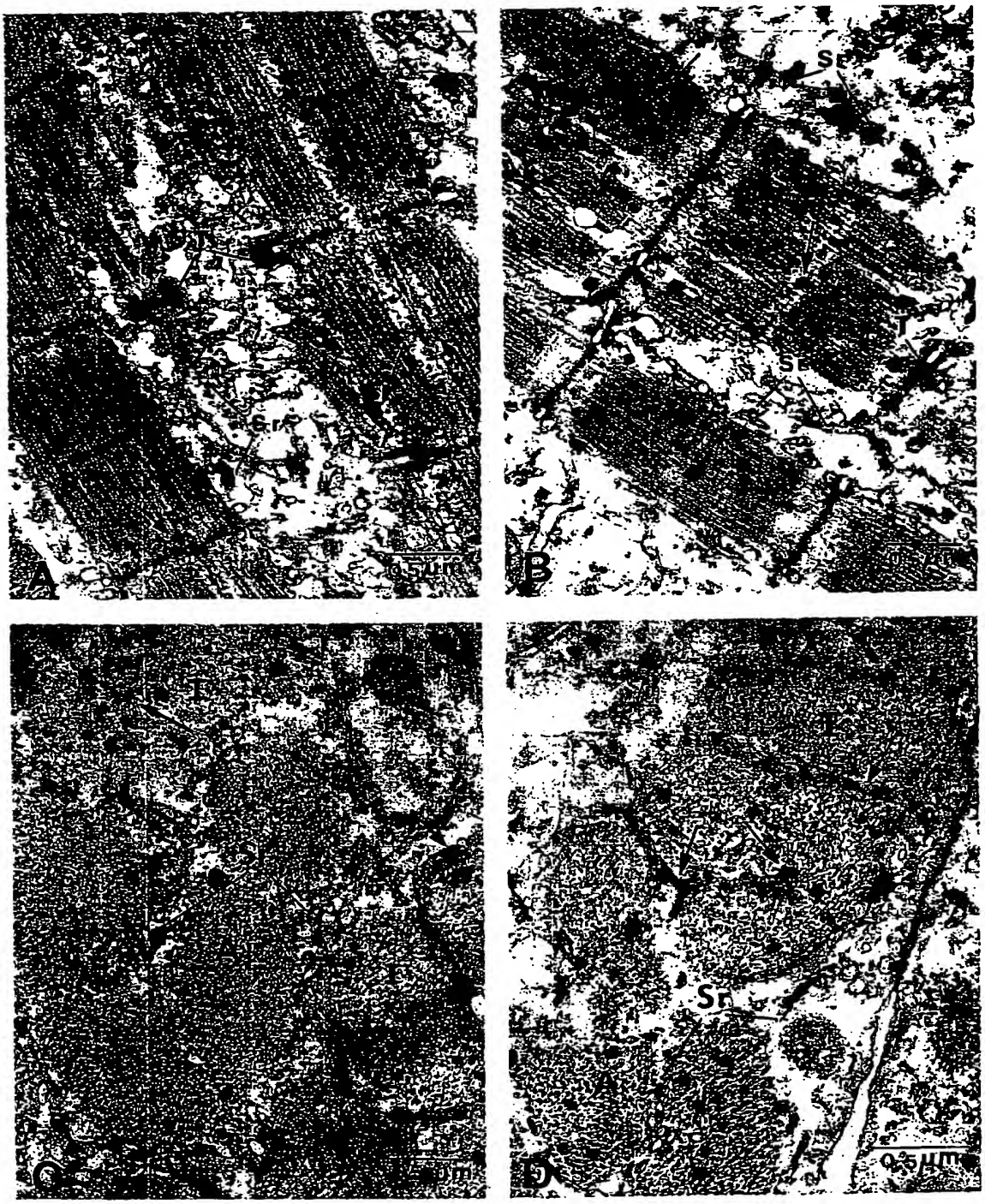

FIG. 6. Overexpression of AChE in myotomes of CMVACHE-injected embryos persists to day 3. Analyses were as in Fig. 5 except that embryos were analyzed after incubation for 3 days. Note the developmental increases in myotomal AChE in both control uninjected (A and C) and CMVACHE-injected sections (B and D), especially within the sarcoplasmic reticulum (Sr) and T-tubules (T). Bar = 0.5 μm.

Aziz-Aloya et al., 1993). To examine the persistence of this state and its implications for synaptic ultrastructure, we studied both cytochemically stained and closely appositioned unstained NMJs from 3-day-old injected and control embryos (Fig. 7 and Table 2). In the injected group, 72% of the postsynaptic membrane length (Table 2) was stained, on average, for active AChE. In contrast, only 22% of the p stsynaptic length was stained in controls. Moreover, the total area covered by reaction product was approximately

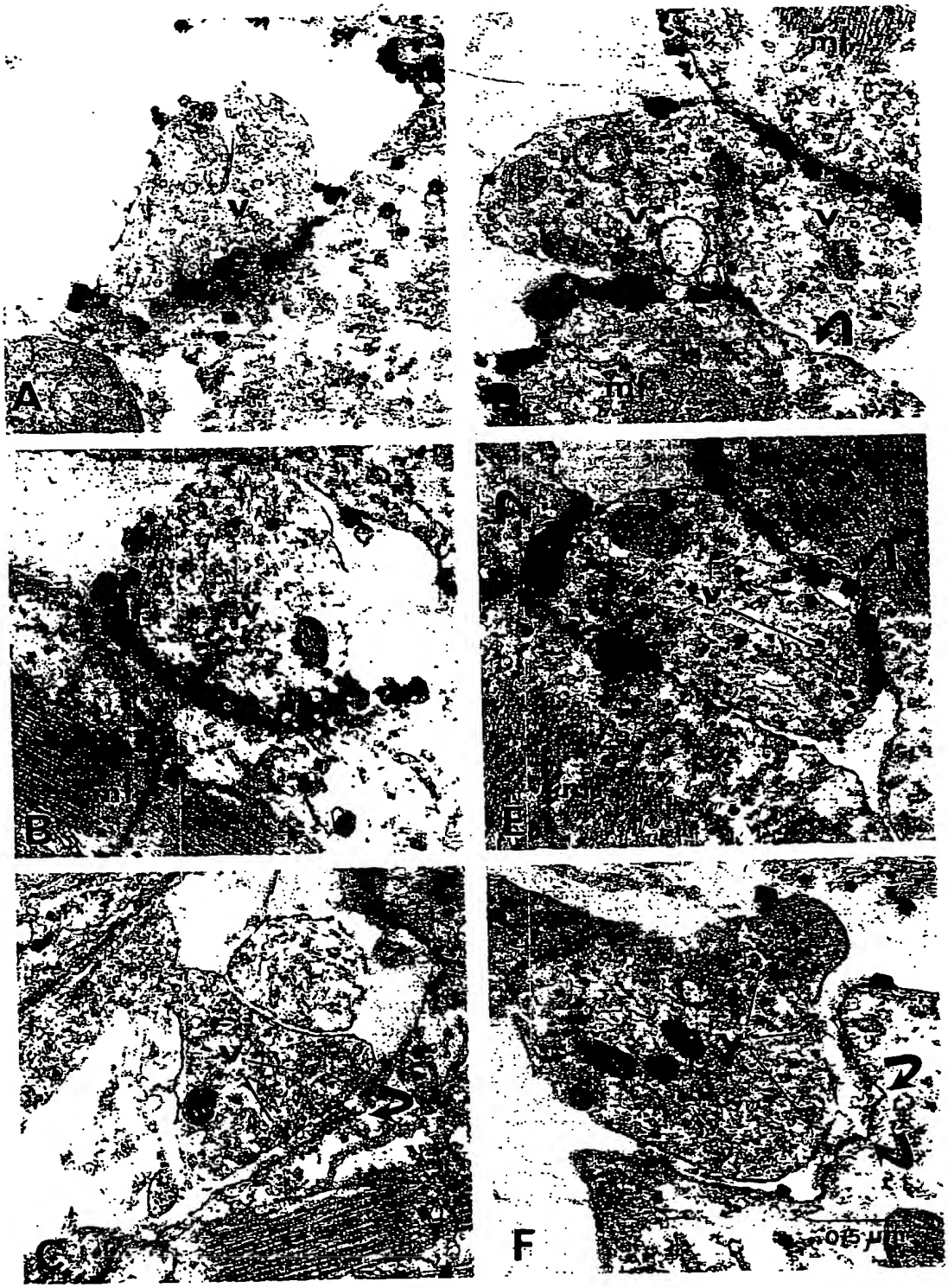

FIG. 7. Structural features in NMJs of 3-day-old CMVACHE-injected *Xenopus* embryos overexpressing AChE. *Xenopus* embryos were cultured for 3 days, fixed, stained for AChE catalytic activity, and examined by transmission electron microscopy as described in Materials and Methods. Two cytochemically stained synapses are presented from uninjected control (A and B) and CMVACHE-injected (D and E) embryos. Note the particularly high-density staining in areas directly opposite nerve terminal zones enriched in presynaptic neurotransmitter vesicles (v). C and F: R presentative unstained NMJs from a control and a CMVACHE-injected embryo, respectively. The synapse shown in B represents the highest degree of staining observed in a control section. mf, myofibril. Arrows indicate postsynaptic folds.

TABLE 2. *Overexpression of AChE in NMJs of 3-day-old CMVACHE-injected* Xenopus *embryos*

Experiment	PSL (μm)	SL (μm)	SL/PSL rati	SA (μm²)
Uninjected	2.57	0.79	0.004	0.156
	3.95	0.79	0.200	0.126
	1.54	0.80	0.060	0.080
	2.35	0.73	0.310	0.082
	1.17	0.44	0.085	0.063
	1.60	0.29	0.180	0.056
	1.02	0.29	0.280	0.040
	0.88	0.58	0.650	0.075
Average ± SD	1.88 ± 0.93	0.58 ± 0.22	0.22 ± 0.19	0.084 ± 0.038
+ CMVACHE	1.76	1.17	0.660	0.284
	2.50	2.05	0.820	0.331
	2.64	1.91	0.720	0.285
	2.50	2.40	0.960	0.476
	3.50	2.03	0.580	0.396
	1.85	1.66	0.900	0.333
	3.10	1.85	0.600	0.535
	3.23	1.76	0.540	0.289
Average ± SD	2.64 ± 0.58	1.85 ± 0.33	0.72 ± 0.15	0.37 ± 0.09
p	<0.01	<0.002	<0.002	<0.002

Eight representative synapses from CMVACHE-injected or control uninjected embryos were assessed for postsynaptic membrane length (PSL), the sum total length covered by reaction product (SL), the fraction of nerve–muscle contact distance displaying reaction product (SL/PSL), and the total stained area (SA). Average ± SD values are given. Measurements were performed on electron micrographs using a hand-held mapping device.

fourfold greater in NMJs from CMVACHE-injected embryos than those from controls (Table 2). In addition, the staining observed in NMJs from injected embryos was considerably more intense than that displayed by control NMJs, forming large black accumulations of reaction product as opposed to the lighter, more diffuse staining observed in controls (Fig. 7A, B, D, and E).

Ultrastructural features of NMJs from injected and uninjected embryos were best discerned in unstained synapses. NMJs from control embryos generally appeared smooth and relatively undeveloped, with up to two secondary folds of the postsynaptic membrane and a single nerve–muscle contact (Fig. 7C). In contrast, NMJs from CMVACHE-injected embryos displayed an average of three secondary folds and one to three discrete contacts between pre- and postsynaptic membranes (Fig. 7F). Furthermore, the average postsynaptic membrane length in NMJs from CMVACHE-injected embryos was 30% larger and considerably less variable than that measured in control embryos (SL; Table 2). Yet, the distance across the synaptic cleft was both larger and more variable in injected embryos than in controls (129 ± 72 vs. 94 ± 23 nm; n = 14). NMJs overexpressing rHAChE thus appeared more developed in their structural buildup than controls.

DISCUSSION

Numerous important nervous system proteins have been expressed in DNA- and RNA-injected oocytes of *X. laevis* (reviewed by Soreq and Seidman, 1992). To study the role and regulation of specific gene products in embryonic development (Vize et al., 1991) and myogenesis (Hopwood et al., 1991), microinjected *Xenopus* embryos have been used. Here, we used microinjected oocytes to demonstrate the efficacy of the CMV promoter in *Xenopus*, observing five- to 10-fold higher levels of heterologous enzyme than that induced by microinjection of in vitro-transcribed mRNA. Although no direct interactions between rHAChE and endogenous *Xenopus* AChE catalytic or structural subunits were observed, calculations of *Xenopus* AChE levels in microinjected embryos indicated that some feedback regulation may be operative in repressing endogenous AChE biosynthesis under conditions of overexpression. Feedback regulation of AChE has been previously demonstrated in chicken retinospheroids (Willbold and Layer, 1992).

Ectopic gene expression/overexpression often results in gross morphogenic aberrations (Harvey and Melton, 1988; McMahon and Moon, 1989; Sokol et al., 1991). Yet, we found that *Xenopus* embryos can tolerate large excesses of catalytically active heterologous AChE without suffering gross morphological or developmental abnormalities. This observation is especially interesting in light of evidence implicating AChE in the early embryonic development of noncholinergic tissues (Drews, 1975) and with developmental processes such as gastrulation and cell migration (Drews, 1975; Fitzpatrick-McElligot and Stent, 1981), nerve outgrowth and differentiation (Layer,

1991), and proliferation and differentiation of hematopoietic cells (Lapidot-Lifson et al., 1989, 1992; Patinkin et al., 1990). As neither the overall rate of development nor general morphology of CMVACHE-injected embryos was altered by 50–100-fold excesses of the active enzyme at the gastrula stage, our findings do not support a role for rHAChE in modulating cell growth, proliferation, or movement in very early *Xenopus* embryogenesis. However, because these biological activities may be unassociated with acetylcholine hydrolysis, they may demonstrate species specificity and remain undetected in our system.

Despite their lack of MyoD elements, some constructs carrying the pan-active CMV promoter (Schmidt et al., 1990) were shown to be expressed in myotomes of transgenic mouse embryos (Kothary et al., 1991). Therefore, the characteristic subcellular segregation of overexpressed rHAChE in muscle may reflect either tissue-specific biosynthesis or posttranslational processing of nascent enzyme present in myotomal progenitor cells at the onset of myogenesis. The high levels of rHAChE present in gastrula-stage embryos may argue for the latter possibility. In that case, the cytochemical data indicate the existence of an intrinsic, evolutionarily conserved property directing the subcellular trafficking of AChE in muscle and thus explain the accumulation of rHAChE in NMJs of ACHE DNA-injected embryos. Furthermore, these results may imply that cotranslational processes are not required for the correct compartmentalization of AChE in muscle cells. In a similar vein, purified recombinant synapsin was shown to be incorporated into synaptic nerve terminals of cultured myotomes following microinjection into fertilized *Xenopus* eggs (Lu et al., 1992).

The general state of myotomal overexpression induced by microinjection of CMVACHE persisted at least 3 days. The area covered by reaction product in cytochemically stained NMJs from day 3, CMVACHE-injected embryos was four- to fivefold over that observed in controls. This figure represents a twofold lower excess than that measured in day 2 NMJs (Ben Aziz-Aloya et al., 1993) yet is slightly greater than the ratio of rHAChE to frog AChE as determined in homogenates at day 3 (Fig. 3A). This apparent reduction in the level of synaptic overexpression from day 2 to day 3 PF may reflect the overall decline in total rHAChE activity observed during this period. However, because this calculation does not consider the higher-density staining observed in NMJs from CMVACHE-injected embryos, it represents an underestimate of the actual synaptic AChE content. Therefore, our data indicate enhanced stability of rHAChE at the NMJ compared with the total pool, a conclusion consistent with the observation that extracellular matrix-associated AChE persists in situ long after denervation of adult frog skeletal muscle (Anglister and McMahan, 1985).

Mammalian cells cotransfected with cDNAs encoding catalytic and noncatalytic AChE subunits (Krejci et al., 1991) produce multimeric globular and asymmetric AChEs, indicating that spatial coexistence may normally be the only requirement for multimeric assembly. Human cell lines transfected with various CMVACHE constructs similarly express and secrete homooligomers (Velan et al., 1991*a*; Kronman et al., 1992). rHAChE displayed oligomeric assembly in microinjected *Xenopus* oocytes but not in developing embryos, where only monomeric rHAChE was detected. Nonetheless, rHAChE was found to accumulate in its natural subcellular compartments and was correctly transported to the NMJ of transiently transfected tadpoles. These findings are puzzling in light of the demonstration that secretion appears linked to oligomerization in transfected human 293 cells (Velan et al., 1991*b*; Kerem et al., 1993). Furthermore, the lack of demonstrable oligomeric assembly leaves the mode of association of rHAChE with the extracellular surface unexplained. It is noteworthy, however, that DNA constructs encoding the parallel AChE form from *Torpedo* (Duval et al., 1992) and the rat (Legay et al., 1993) also gave rise to globular amphiphilic AChE forms in transfected mammalian cells, including type II amphiphilic monomers.

In humans, ultrastructural and physiological alterations of the NMJ have been associated with congenital AChE and AChR deficiencies (Wokke et al., 1989; Jennekens et al., 1992) and may be associated with changes in the balance between these two molecules at the synapse. In one of these syndromes, patients presented, in addition to AChE/AChR deficits, NMJs displaying decreased miniature end-plate potentials, reduced postsynaptic membrane lengths, and severely impaired postsynaptic secondary folding (Smit et al., 1988)—opposite features to those observed in our NMJs overexpressing AChE. It is yet unclear whether the reduced expression of synaptic AChE and/or AChR represents a cause or an outcome of the ultrastructural aberrations observed in these patients. Our current observations suggest that disturbed regulation of AChE may, indeed, carry ultrastructural consequences for synaptic development. It will thus be interesting to assess the impact of AChE overexpression on the expression and organization of AChR and other key synaptic proteins in these transiently transgenic tadpoles.

Acknowledgment: We are grateful to Dr. J. Yisraeli, Hadassah Medical School, Jerusalem, Israel, for guidance in the embryo microinjections. This research was supported by the U.S. Army Medical Research and Development Command (grant DAMD 17-90-Z0038), the United States–Israel Binational Science Foundation (grant 89-00205), and the Israel Science Foundation administered by the Israel Academy of Sciences and Humanities (to H.S.). J.L. was a recipient of a short-term EMBO fellowship.

REFERENCES

Anglister L. and McMahan U. J. (1985) Basal lamina directs acetylcholinesterase accumulati n at synaptic sites in regenerating muscle. *J. Cell Biol.* **101**, 735–743.

Ben Aziz-Aloya R., Seidman S., Timberg R., Sternfeld M., Zakut H., and Soreq H. (1993) Expression of a human acetylcholinesterase prom ter-reporter construct in developing neuromuscular junctions of *Xenopus* embryos. *Proc. Natl. Acad. Sci. USA* **90**, 2471–2475.

Brandan E., Maldonado M., Garrido J., and Inestrosa N. C. (1985) Anchorage of collagen-tailed acetylcholinesterase is mediated by heparan sulfate proteoglycans. *J. Cell Biol.* **101**, 985–992.

Brodbeck U. and Liao J. (1992) Subunit assembly and glycosylation of acetylcholinesterase from mammalian brain, in *Multidisciplinary Approaches to Cholinesterase Functions* (Shafferman A. and Velan B., eds), pp. 33–38. Plenum Press, New York.

Changeux J. P. (1991) Compartmentalized transcription of acetylcholine receptor genes during motor endplate epigenesis. *New Biol.* **3**, 413–429.

Cohen M. W. (1980) Development of an amphibian neuromuscular junction *in vivo* and in culture. *J. Exp. Biol.* **89**, 43–56.

Deuchar E. M. (1966) *Biochemical Aspects of Amphibian Development.* Methuen and Co. Ltd., London.

Drews U. (1975) Cholinesterase in embryonic development. *Prog. Histochem. Cytochem.* **7**, 1–52.

Duval N., Massoulie J., and Bon S. (1992) H and T subunits of acetylcholinesterase from *Torpedo*, expressed in COS cells, generate all types of molecular forms. *J. Cell Biol.* **118**, 641–653.

Fitzpatrick-McElligot S. and Stent G. S. (1981) Appearance and localization of acetylcholinesterase in embryos of the leech *Helodbella triserialis*. *J. Neurosci.* **1**, 901–907.

Flucher B. E. and Daniels M. D. (1989) Distribution of Na^+ channels and ankyrin in neuromuscular junctions is complementary to that of acetylcholine receptors and the 43 Kd protein. *Neuron* **3**, 163–175.

Froehner S. C. (1991) The submembrane machinery for nicotinic acetylcholine receptor clustering. *J. Cell Biol.* **114**, 1–7.

Gennari K. and Brodbeck U. (1985) Molecular forms of acetylcholinesterase from human caudate nucleus: comparison of salt-soluble and detergent-soluble tetrameric enzyme species. *J. Neurochem.* **44**, 697–704.

Gindi T. and Knowland J. (1979) The activity of cholinesterases during the development of *Xenopus laevis*. *J. Embryol. Exp. Morphol.* **51**, 209–215.

Hall Z. W. (1973) Multiple forms of acetylcholinesterase and their distribution in endplate and non-endplate regions of rat diaphragm muscle. *J. Neurobiol.* **4**, 343–361.

Harvey R. P. and Melton D. A. (1988) Microinjection of synthetic Xhox-1A homeobox mRNA disrupts somite formation in developing *Xenopus* embryos. *Cell* **53**, 687–697.

Hopwood N. D., Pluck A., and Gurdon J. B. (1991) *Xenopus* Myf-5 marks early muscle cells and can activate muscle genes ectopically. *Development* **111**, 551–560.

Jennekens F. G. I., Hesselmans L. F. G. M., Veldman H., Jansen E. N. H., Spaans F., and Molenaar P. C. (1992) Deficiency of acetylcholine receptors in a case of end-plate acetylcholinesterase deficiency: a histochemical investigation. *Muscle Nerve* **15**, 63–72.

Karnovsky M. J. (1964) The localization of cholinesterase activity in rat cardiac muscle by electron microscope. *J. Cell Biol.* **23**, 217–232.

Kerem A., Kronman C., Bar-Nun S., Shafferman A., and Velan B. (1993) Interaction between assembly and secretion of recombinant human acetylcholinesterase. *J. Biol. Chem.* **268**, 180–184.

Kothary R., Barton S. C., Franz T., Norris M. L., Hettle S., and Surani A. M. H. (1991) Unusual cell specific expression of a major human cytomegalovirus immediate early gene promoter–lacZ hybrid gene in transgenic mouse embryos. *Mech. Dev.* **35**, 25–31.

Krejci E., Coussen F., Duval N., Chatel J.-M., Legay C., Puype M., Vandekerckhove J., Cartaud J., Bon S., and Massoulie J. (1991) Primary structure of a collagenic tail peptide of *Torpedo* acetylcholinesterase: co-expression with catalytic subunit induces the production of collagen-tailed forms in transfected cells. *EMBO J.* **10**, 1285–1293.

Kronman C., Velan B., Gozes Y., Leitner M., Flashner Y., Lazar A., Marcus D., Sery T., Papier A., Grosfeld H., Cohen S., and Shafferman A. (1992) Production and secretion of high levels of recombinant human acetylcholinesterase in cultured cell lines: microheterogeneity of the catalytic subunit. *Gene* **121**, 295–304.

Kullberg R. W., Lentz T. L., and Cohen M. W. (1977) Development of the myotomal neuromuscular junction in *Xenopus laevis*: an electrophysiological and fine-structural study. *Dev. Biol.* **60**, 101–129.

Kullberg R. W., Mikelberg F. S., and Cohen M. W. (1980) Contribution of cholinesterase to developmental decreases in the time course of synaptic potentials at an amphibian neuromuscular junction. *Dev. Biol.* **75**, 255–267.

Lapidot-Lifson Y., Prody C. A., Ginzberg D., Meytes D., Zakut H., and Soreq H. (1989) Co-amplification of human acetylcholinesterase and butyrylcholinesterase in blood cells: correlation with various leukemias and abnormal megakaryocytopoiesis. *Proc. Natl. Acad. Sci. USA* **86**, 4715–4717.

Lapidot-Lifson Y., Patinkin D., Prody C., Ehrlich G., Seidman S., Ben-Aziz R., Eckstein F., Benseler F., Zakut H., and Soreq H. (1992) Cloning and antisense oligodeoxynucleotide inhibition of a human homolog of cdc2 required in hematopoiesis. *Proc. Natl. Acad. Sci. USA* **89**, 579–583.

Layer P. (1991) Cholinesterases during avian development. *Cell. Mol. Neurobiol.* **11**, 7–34.

Legay C., Bon S., Vernier P., Coussen F., and Massoulié J. (1993) Cloning and expression of a rat acetylcholinesterase subunit: generation of multiple molecular forms, complementarity with a *Torpedo* collagenic subunit. *J. Neurochem.* **60**, 337–346.

Liao J., Heider H., Sun M.-C., and Brodbeck U. (1992) Different glycosylation in acetylcholinesterases from mammalian brain and erythrocytes. *J. Neurochem.* **58**, 1230–1238.

Lu B., Greengard P., and Poo M. (1992) Exogenous synapsin I promotes functional maturation of developing neuromuscular synapses. *Neuron* **8**, 521–529.

McMahan U. J. (1990) The agrin hypothesis. *Cold Spring Harb. Symp. Quant. Biol.* **55**, 407–418.

McMahon A. P. and Moon R. T. (1989) Ectopic expression of the proto-oncogene int-1 in *Xenopus* embryos leads to duplication of the embryonic axis. *Cell* **58**, 1075–1084.

Neville L. F., Gnatt A., Loewenstein Y., Seidman S., Ehrlich G., and Soreq H. (1992) Intra-molecular relationships in cholinesterases revealed by oocyte expression of site-directed and natural variants of human BCHE. *EMBO J.* **11**, 1641–1649.

Ohlendieck K., Ervasti J. M., Matsumura K., Kahl S. D., Leveille C. J., and Campbell K. P. (1991) Dystrophin-related protein is localized to neuromuscular junctions of adult skeletal muscle. *Neuron* **7**, 499–508.

Patinkin D., Seidman S., Eckstein F., Benseler F., Zakut H., and Soreq H. (1990) Manipulations of cholinesterase gene expression modulate murine megakaryocytopoiesis *in vitro*. *Mol. Cell. Biol.* **10**, 6046–6050.

Pavlath G. K., Rich K., Webster S. G., and Blau H. M. (1989) Localization of muscle gene products in nuclear domains. *Nature* **337**, 570–573.

Phillips W. D., Kopta C., Blount P., Gardner P. D., Steinbach J. H., and Merlie J. P. (1991) ACh receptor-rich membrane domains organized in fibroblasts by recombinant 43 kilodalton protein. *Nature* **251**, 568–570.

Ralston E. and Hall Z. W. (1989) Transfer of a protein encoded by a single nucleus to nearby nuclei in multinucleated myotubes. *Nature* **244**, 1066–1069.

Rossi S. G. and Rotundo R. L. (1992) Cell surface acetylcholinesterase molecules on multinucleated myotubes are clustered over the nucleus of origin. *J. Cell Biol.* **119**, 1657–1667.

Rotundo R. L. (1990) Nucleus-specific translation and assembly of

acetylcholinesterase in multinucleated muscle cells. *J. Cell Biol.* **110**, 715–719.

Schmidt E. V., Christoph G., Zeller R., and Leder P. (1990) The cytomegalovirus enhancer: a Pan-active control element in transgenic mice. *Mol. Cell. Biol.* **10**, 4406–4411.

Smit L. M. E., Hageman G., Veldman H., Molenaar P. C., Oen B. S., and Jennekens F. G. I. (1988) A myasthenic syndrome with congenital paucity of secondary clefts: CPSC syndrome. *Muscle Nerve* **11**, 337–348.

Sokol S., Christian J. L., Moon R. T., and Melton D. A. (1991) Injected Wnt RNA induces a complete body axis in *Xenopus* embryos. *Cell* **67**, 741–752.

Soreq H. and Seidman S. (1992) *Xenopus* oocyte microinjection: from gene to protein, in *Methods in Enzymology* (B. Rudy and L. Iversen, eds), pp. 225–265. Academic Press, San Diego.

Soreq H., Seidman S., Dreyfus P. A., Zevin-Sonkin D., and Zakut H. (1989) Expression and tissue specific assembly of cloned human butyrylcholine esterase in microinjected *Xenopus laevis* oocytes. *J. Biol. Chem.* **264**, 10608–10613.

Soreq H., Ben-Aziz R., Prody C., Seidman S., Gnatt A., Neville L., Lieman-Hurwitz J., Lev-Lehman E., Ginzberg D., Lapidot-Lifson Y., and Zakut H. (1990) Molecular cloning and construction of the coding region for human acetylcholinesterase reveals a G,C rich attenuating structure. *Proc. Natl. Acad. Sci. USA* **87**, 9688–9692.

Velan B., Kronman C., Grosfeld H., Leitner M., Gozes Y., Flashner Y., Sery T., Cohen S., Ben-Aziz R., Seidman S., Shafferman A., and Soreq H. (1991*a*) Recombinant human acetylcholinesterase is secreted from transiently transfected 293 cells as a soluble globular enzyme. *Cell. Mol. Neurobiol.* **11**, 143–156.

Velan B., Grosfeld H., Kronman C., Leitner M., Gozes Y., Lazar A., Flashner Y., Marcus D., Cohen S., and Shafferman A. (1991*b*) The effect of elimination of intersubunit disulfide bonds on the activity, assembly, and secretion of recombinant human acetylcholinesterase. *J. Biol. Chem.* **266**, 23977–23984.

Vize P. D., Melton D. A., Hemmati-Brivanlou A., and Harland R. M. (1991) Assays for gene function in developing *Xenopus* embryos, in *Methods in Cell Biology* (Kay B. K. and Peng H. B., eds), pp. 367–387. Academic Press, San Diego.

Wallace B. G. (1991) The mechanisms of agrin-induced acetylcholine receptor aggregation. *Philos. Trans. R. Soc. Lond. Biol.* **331**, 272–280.

Willbold E. and Layer P. (1992) Formation of neuroblastic layers in chicken retinospheroids: the fibre layer of Chievitz secludes AChE positive cells from mitotic cells. *Cell Tissue Res.* **268**, 401–408.

Wokke J. H. J., Jennekens F. G. I., Molenaar P. C., Van den Oord C. J. M., Oen B. S., and Busch H. F. M. (1989) Congenital paucity of secondary synaptic clefts (CPSC) syndrome in 2 adult siblings. *Neurology* **38**, 648–654.